Mineralogical Magazine, June 2014, Vol. 78(3), pp. 651–661

Lead-antimony sulfosalts from Tuscany (Italy). XV. (Tl-Ag)-bearing rouxelite from Monte Arsiccio mine: occurrence and crystal chemistry

C. Biagioni[1,*], Y. Moëlo[2] and P. Orlandi[1,3]

[1] Dipartimento di Scienze della Terra, Università di Pisa, Via S. Maria 53, I-56126 Pisa, Italy
[2] Institut des Matériaux Jean Rouxel, UMR 6502, CNRS, Université de Nantes, 2, rue de la Houssinière, 44322 Nantes Cedex 3, France
[3] Istituto di Geoscienze e Georisorse, CNR, Via Moruzzi 1, I-56124 Pisa, Italy

[*Received 28 November 2013; Accepted 25 February 2014; Associate Editor: A. Christy*]

ABSTRACT

A third world occurrence of rouxelite, ideally $Cu_2HgPb_{22}Sb_{28}S_{64}(O,S)_2$, has been identified from the baryte-pyrite-Fe oxides ore of Monte Arsiccio mine, near Sant'Anna di Stazzema (Apuan Alps, Tuscany, Italy). Rouxelite occurs as mm-sized acicular crystals, black in colour, with bluish-violet iridescence, in vugs of carbonate + baryte + quartz veins embedded in dolostones from the Sant'Olga tunnel. It is associated with Tl-bearing chovanite, sphalerite and valentinite. Its X-ray powder diffraction pattern gives unit-cell parameters $a = 43.10(2)$, $b = 4.060(2)$, $c = 37.88(2)$ Å, $\beta = 117.33(2)^{\circ}$, $V = 5889(5)$ Å^3. Electron-microprobe data reveal a complex chemistry, with additional minor elements (wt.%): Tl (0.6−1.7), Ag (0.4−0.6), As (0.2−0.6) and Bi ($\leqslant$0.05). This indicates a widespread substitution of Hg by Ag, according to Hg + Pb = Ag + Sb and incorporation of Tl, with some Ag, according to 2Pb = Sb + (Tl, Ag). The occurrence of mixed (Hg, Ag) and (Hg, Cu) sites in natural sulfides and sulfosalts is briefly reviewed. The Tl-content of the samples studied is a characteristic fingerprint agreeing with the Tl-rich nature of the mineral assemblage from Monte Arsiccio. Rouxelite therefore constitutes a new example of a Tl-bearing sulfosalt.

Keywords: rouxelite, mercury, silver, thallium, sulfosalt, Monte Arsiccio mine, Apuan Alps, Tuscany, Italy.

Introduction

Rouxelite is a complex Pb-Sb sulfosalt first described by Orlandi *et al*. (2005) from the baryte-pyrite-Fe oxides ore deposit of Buca della Vena, Apuan Alps, Tuscany, Italy. At the type locality, rouxelite is very rare and occurs as very thin, black, acicular crystals elongated on [010]. In the type description, the authors reported the identification of a second occurrence of rouxelite from the Sb deposit of Magurka, Slovakia. The Slovak rouxelite is characterized by a smaller Hg content compensated by a significant Ag content, with respect to rouxelite from Buca della Vena.

In the last few years, mineralogical research has been extended to other baryte-pyrite-Fe oxides deposits in the southern Apuan Alps, with the discovery of several interesting mineral species. In particular, Ag-Pb/Sb-As sulfosalts have been described from the Pollone mine (sterryite, parasterryite, carducciite and meerschautite; Moëlo *et al*., 2011; Biagioni *et al*., 2013*c*,*d*), whereas a more complex sulfosalt assemblage has been found at the Monte Arsiccio mine, with the description of Hg-Tl-Pb-Sb-As-Cu-Ag sulfides and sulfosalts (e.g. Biagioni *et al*., 2013*b*). In the latter assemblage a third occurrence of rouxelite was identified. Additional chemical

* E-mail: biagioni@dst.unipi.it
DOI: 10.1180/minmag.2014.078.3.13

data on this Pb-Sb sulfosalt was collected showing a very interesting crystal-chemical complexity. The aim of this short paper is the description of this new rouxelite occurrence and its full chemical characterization.

Geological setting and occurrence of rouxelite

The baryte-pyrite-Fe oxides deposit of Monte Arsiccio (43º58′N, 10º17′E) is located in the northeastern portion of the Sant'Anna tectonic window, an area in which outcrops of metamorphic rocks are surrounded by the non-metamorphic sedimentary formations of the overlying Tuscan Nappe. The geological setting of this locality has been discussed by previous authors (e.g. Costagliola *et al*., 1990; Orlandi *et al*., 2012).

Interesting sulfosalt assemblages have been found at the Sant'Olga tunnel (525 m a.s.l.), in an area where a dolostone lens edges the quartz-muscovite schist footwall belonging to the Scisti di Fornovolasco Formation (Pandeli *et al*., 2004). Sulfosalts have been found in three different occurrences: (1) microcrystalline baryte + pyrite, at the contact between schist and dolostone; (2) pyrite-rich dolostones, near the contact with the schists; and (3) carbonate + baryte + quartz veins embedded in the dolostone. Table 1 summarizes the different sulfide and sulfosalt assemblages identified in these three kinds of occurrence. Rouxelite has been found in the third type, i.e. in carbonate + baryte + quartz veins. This kind of occurrence has provided a series of idiomorphic mineral species, represented in particular by acicular Pb-Sb sulfosalts in the vugs of the veins (Fig. 1). The most common phase is probably zinkenite, whereas jamesonite, robinsonite, rouxelite and chovanite are very rare; moreover, boulangerite is rather uncommon. In the same veins, yellow to orange-red tetrahedral or pseudo-octahedral crystals of sphalerite, up to 1 cm and mm-sized tetrahedral crystals of tetrahedrite have been found. Energy-dispersive

TABLE 1. Sulfides and sulfosalts identified in mineral assemblages from the Sant'Olga tunnel.

Mineral species	Chemical formula	Brt + Py	Dol	Veins
Arsiccioite	$AgHg_2TlAs_2S_6$	X		
Aktashite	$Cu_6Hg_3As_4S_{12}$		X	
Boscardinite	$TlPb_4(Sb,As)_9S_{18}$		X	X
Boulangerite	$Pb_5Sb_4S_{11}$			X
Cinnabar	HgS	X		
Chovanite	$Pb_{15-2x}Sb_{14+2x}S_{36}O_x$			X
Jamesonite	$FePb_4Sb_6S_{14}$			X
Laffittite	$AgHgAsS_3$	X	X	
Polhemusite?	(Zn,Hg)S	X		
Protochabournéite	$Tl_2Pb(Sb_{9-8}As_{1-2})_{\Sigma 10}S_{17}$	X	X	X
"Quatrandorite"	$CuHgAg_7Pb_7(Sb,As)_{24}S_{48}$			X
Realgar	As_4S_4	X	X	X
Robinsonite	$Pb_4Sb_6S_{13}$			X
Routhierite	$CuHg_2TlAs_2S_6$		X	X
Rouxelite	$Cu_2HgPb_{22}Sb_{28}S_{64}(O,S)_2$			X
Sphalerite	ZnS	X	X	X
Stibnite	Sb_2S_3	X	X	X
Tetrahedrite	$Cu_6[Cu_4(Fe,Zn)_2]Sb_4S_{13}$			X
Twinnite	$Pb(Sb,As)_2S_4$		X	
Zinkenite	$Pb_9Sb_{22}S_{42}$		X	X

Chemical formulae after Moëlo *et al*. (2008), with the exception of the recently described mineral species arsiccioite (Biagioni *et al*., 2014), boscardinite (Orlandi *et al*., 2012), chovanite (Topa *et al*., 2012) and protochabournéite (Orlandi *et al*., 2013). "Quatrandorite" is currently under study. Minerals for which the type locality is Monte Arsiccio are given in bold.

The three kinds of occurrences are labelled as: Brt + Py = microcrystalline baryte + pyrite; Dol = pyrite-rich dolostone; Veins = carbonate + baryte + quartz veins.

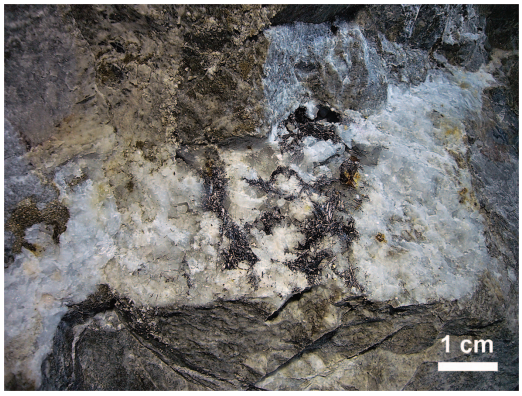

FIG. 1. Carbonate + baryte + quartz vein embedded in the dolostone, with cavities filled by acicular Pb-Sb sulfosalts and yellow crystals of sphalerite. Sant'Olga tunnel.

spectrometry qualitative chemical analysis showed a detectable Hg content in these mineral species. In some cases, white to yellow tabular crystals or hemispherical aggregates of valentinite, up to 5 mm, occur.

Mineral description

Rouxelite was identified in less than ten specimens. It occurs as acicular crystals, deeply striated along [010], black in colour with bluish-violet tints (Fig. 2). This iridescence probably relates to a microscopic oxidation film, as observed in other sulfosalts from the same locality (e.g. zinkenite) and from Buca della Vena mine (e.g. scainiite, Orlandi *et al*., 1999). The maximum size of the crystal aggregates, formed by the parallel association of acicular individuals, is ~5 mm. In the studied specimens, rouxelite is associated with Tl-bearing chovanite, sphalerite and valentinite.

X-ray diffraction data

The identification of rouxelite is based on X-ray powder diffraction (XRPD) data collected using a 114.6 mm Gandolfi camera and Ni-filtered Cu$K\alpha$ radiation. Table 2 compares the X-ray diffraction lines observed for rouxelite from Monte Arsiccio (sample #318) with those reported by Orlandi *et al*. (2005) for the type locality. The agreement between the two datasets is good. Only one relatively broad peak at 3.393 Å occurs in the XRPD pattern collected on sample #318, whereas

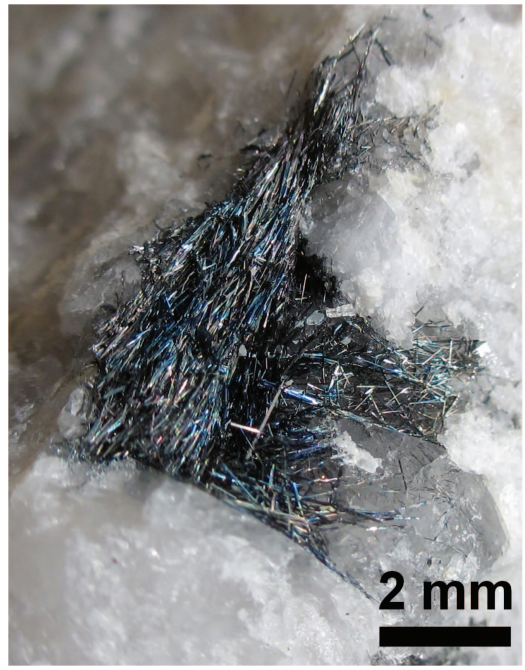

FIG. 2. Rouxelite, acicular crystals up to 5 mm, with a bluish iridescence in a cavity of a carbonate + baryte + quartz vein. Sant'Olga tunnel. Specimen #399.

in rouxelite from Buca della Vena, two strong peaks were observed at 3.402 and 3.369 Å. The reflections at 3.596 and 3.556 Å, observed in the XRPD pattern of Monte Arsiccio, were not reported by Orlandi *et al*. (2005); actually, these two diffractions correspond to those at 3.589 and 3.538 Å in the calculated XRPD pattern of rouxelite, having relative intensities 17 and 10, respectively. On the contrary, the very weak reflections at 2.481 and 2.309 Å reported by Orlandi *et al*. (2005) do not occur in the pattern of sample #318, but were observed in the XRPD collected on another sample (#399). Figure 3 compares the XRPD patterns of rouxelite from Monte Arsiccio with that of a sample from the type locality. Unit-cell parameters, refined through the software *Celref* (Laugier and Bochu, 1999), are a = 43.10(2), b = 4.060(2), c = 37.88(2) Å, β = 117.33(2)º, V = 5889(5) Å^3, almost identical to the cell constants given by Orlandi *et al*. (2005): a = 43.113(9), b = 4.0591(8), c = 37.874(8) Å, β = 117.35(3)º, V = 5887(2) Å^3.

Fibrous crystals of rouxelite were selected in order to collect single-crystal X-ray diffraction data using a Bruker Smart Breeze diffractometer

TABLE 2. X-ray powder diffraction data for rouxelite (sample #318), compared with the X-ray powder data given by Orlandi *et al*. (2005).

Monte Arsiccio (this work)		Buca della Vena (Orlandi *et al.*, 2005)	
I_{obs}	d_{obs}	I_{obs}	d_{obs}
–	–	16	10.40
–	–	10	8.08
–	–	6	5.91
mw	4.195	19	4.19
mw	4.024	17	4.04
mw	3.850	31	3.84
w	3.778	10	3.76
w	3.631	21	3.62
w	3.596	–	–
vw	3.556	–	–
mw	3.503	29	3.509
vs	3.393	100	3.402
		74	3.369
w	3.179	21	3.206
mw	3.055	18	3.068
w	2.987	16	3.009
mw	2.893	28	2.898
ms	2.805	70	2.815
m	2.748	36	2.756
vw	2.667	5	2.673
vw	2.630	8	2.628
vw	2.535	9	2.528
–	–	5	2.481
vw	2.387	6	2.385
w	2.348	12	2.350
–	–	5	2.309
m	2.248	31	2.251
w	2.215	16	2.220
w	2.142	19	2.150
m	2.115	31	2.116
w	2.088	16	2.089
mw	2.040	21	2.040
mw	2.030	–	–
w	1.978	13	1.983
m	1.950	30	1.955
w	1.925	11	1.923
mw	1.878	15	1.888
		15	1.871
mw	1.819	15	1.814
mw	1.810	–	–
mw	1.797	9	1.780
mw	1.736	26	1.743
mw	1.703	16	1.704

Note: observed intensities were estimated visually. vs = very strong; ms = medium–strong; m = medium; mw = medium–weak; w = weak; vw = very weak.

equipped with an air-cooled CCD detector and graphite-monochromated Mo$K\alpha$ radiation. Unfortunately, the selected fibres were discovered to be composed of sub-parallel acicular crystals, giving rise to poor quality diffraction data. Crystals are elongated on the 4 Å axis (**b** direction) and show a weak 2*b* superstructure, in agreement with Orlandi *et al*. (2005).

Chemical analysis

Two samples (samples #318 and #399) were analysed with a CAMEBAX SX100 electron microprobe. The operating conditions were: accelerating voltage 20 kV, beam current 20 nA, beam size 5 μm; standards (element and emission line, counting times for one spot analysis) are: pyrite (S$K\alpha$, 50 s), stibnite (Sb$L\alpha$, 30 s), Ag (Ag$L\alpha$, 30 s), galena (Pb$M\alpha$, 30 s), lorandite (Tl$M\alpha$, 20 s), cinnabar (Hg$M\alpha$, 20 s), Bi (Bi$M\alpha$, 20 s), AsGa (As$L\alpha$, 40 s) and Cu (Cu$K\alpha$, 30 s). Table 3 gives the weight percentages; according to the variability of the minor elements (especially Tl), spot analyses of sample #318 have been classified into three groups (A, B and C), while the fourth group, D, represents sample #399. Totals are good for sample #318, while a significant deficit occurs for sample #399 (average total ~97.4 wt.%), owing to the thinness of the analysed fibre. Nine elements have been detected: major Pb, Sb and S and minor Cu, Ag, Hg, Tl and As; Bi occurs in only four spot analyses. Among the minor elements, four (Ag, Tl, As and Bi) were not detected previously in rouxelite from the type deposit of Buca della Vena, whereas Ag also occurred in the specimen from Magurka (Orlandi *et al*., 2005).

Crystal chemistry of rouxelite

Table 4 gives the chemical formulae recalculated from electron-microprobe analyses on the basis of $\Sigma Me = 53$ atoms per formula unit (a.p.f.u.).

The Cu content fits the ideal ratio of the structural formula very well, i.e. $Cu_2HgPb_{22}Sb_{28}S_{64}(O,S)_2$. A small deficit in analysis D (1.92 a.p.f.u.) is related to the highest Ag content. In this sample, ~0.08 Ag a.p.f.u. probably substitutes for Cu. On the contrary, the small excess of Cu in analysis C (0.04 a.p.f.u.) could substitute for Hg. A negative correlation occurs between (Ag + Cu) (in relative excess compared to the 2 Cu atoms in the structural formula) and Hg (Fig. 4). The sum (Ag + Hg) is

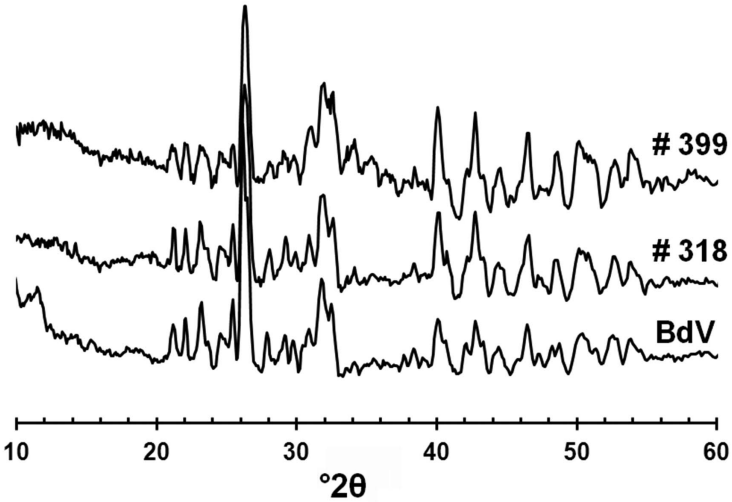

FIG. 3. Comparison between observed XRPD patterns of rouxelite from Monte Arsiccio mine (samples #318 and 399) with those from Buca della Vena mine (BdV).

TABLE 3. Chemical data (wt.%) of rouxelite from Monte Arsiccio. For comparison, the average chemical compositions of rouxelite from Buca della Vena and Magurka are given (from Orlandi *et al*., 2005).

Sample	Spot	Cu	Ag	Hg	Tl	Pb	Sb	As	Bi	S	Total
318	A1	1.20	0.47	1.44	0.62	41.94	32.74	0.43	0.05	20.07	99.18
318	A2	1.23	0.58	1.32	0.54	41.85	32.87	0.49	0.05	20.41	99.56
318	A3	1.27	0.39	1.45	0.62	42.61	33.04	0.49	0.06	20.47	100.62
	Mean A	1.23	0.48	1.40	0.59	42.13	32.88	0.47	0.05	20.32	99.79
318	B1	1.22	0.39	1.58	0.98	41.60	32.71	0.63	0.00	20.47	99.61
318	B2	1.26	0.36	1.45	0.93	42.25	33.20	0.61	0.02	20.42	100.91
	Mean B	1.24	0.37	1.52	0.95	41.93	32.96	0.62	0.01	20.45	100.26
318	C1	1.27	0.38	1.35	1.67	40.59	34.38	0.20	0.06	20.49	100.60
318	C2	1.25	0.40	1.26	1.72	39.05	34.25	0.21	0.03	20.26	98.83
318	C3	1.25	0.44	1.25	1.81	38.69	34.81	0.18	0.02	20.27	99.18
318	C4	1.25	0.45	1.38	1.41	39.65	34.17	0.20	0.00	20.61	98.96
	Mean C	1.26	0.42	1.31	1.65	39.50	34.40	0.20	0.03	20.40	99.39
399	D1	1.14	0.60	1.10	0.91	38.88	32.83	0.46	0.03	20.16	96.33
399	D2	1.20	0.62	1.12	0.88	39.55	33.41	0.48	0.04	20.30	97.83
399	D3	1.16	0.74	1.15	0.95	40.10	33.17	0.48	0.02	20.23	98.24
399	D4	1.12	0.56	1.11	0.85	39.98	32.90	0.52	0.03	19.92	97.21
	Mean D	1.16	0.63	1.12	0.89	39.63	33.08	0.48	0.03	20.15	97.40
Buca della Vena		1.34	–	1.76	–	45.08	31.50	–	–	20.07	99.75
Magurka		1.28	0.35	1.07	–	45.59	31.94	–	–	19.92	100.15

TABLE 4. Chemical formulae (in a.p.f.u.) recalculated on the basis of Σ*Me* = 53 a.p.f.u. Data for rouxelite from Buca della Vena and Magurka are given for comparison (from Orlandi *et al*., 2005). Valence equilibrium: Ev (%) = [Σ(val+) − Σ(val−)] × 100/Σ(val−).

Sample	Spot	Cu	Ag	Hg	Tl	Pb	Sb	As	Bi	S	Ev
318	A1	1.96	0.45	0.75	0.31	21.01	27.91	0.60	0.02	64.97	1.4
318	A2	2.00	0.55	0.68	0.27	20.88	27.92	0.68	0.02	65.83	0.1
318	A3	2.04	0.37	0.74	0.31	21.06	27.79	0.66	0.03	65.36	0.8
	Mean A	2.00	0.46	0.72	0.30	20.98	27.87	0.65	0.03	65.39	0.8
318	B1	1.98	0.37	0.82	0.50	20.73	27.74	0.86	0.00	65.92	–0.1
318	B2	2.03	0.34	0.74	0.46	20.79	27.81	0.83	0.01	64.93	1.5
	Mean B	2.00	0.36	0.78	0.48	20.76	27.78	0.84	0.00	65.43	0.7
318	C1	2.04	0.36	0.69	0.83	19.98	28.80	0.27	0.03	65.17	1.2
318	C2	2.05	0.39	0.65	0.87	19.56	29.18	0.29	0.02	65.54	0.8
318	C3	2.03	0.42	0.64	0.91	19.25	29.48	0.25	0.01	65.17	1.6
318	C4	2.03	0.44	0.71	0.71	19.80	29.04	0.27	0.00	66.50	–0.6
	Mean C	2.04	0.40	0.67	0.83	19.65	29.13	0.27	0.01	65.59	0.7
399	D1	1.92	0.59	0.58	0.47	20.01	28.75	0.66	0.01	67.03	–1.2
399	D2	1.98	0.60	0.59	0.45	19.98	28.72	0.67	0.02	66.24	–0.1
399	D3	1.90	0.72	0.60	0.48	20.19	28.42	0.67	0.01	65.81	0.3
399	D4	1.86	0.54	0.58	0.44	20.35	28.49	0.73	0.01	65.51	1.0
	Mean D	1.92	0.61	0.59	0.46	20.13	28.60	0.68	0.01	66.15	0.0
	Buca della Vena	2.20	–	0.92	–	22.78	27.10	–	–	65.53	
	Magurka	2.08	0.33	0.55	–	22.80	27.24	–	–	64.67	

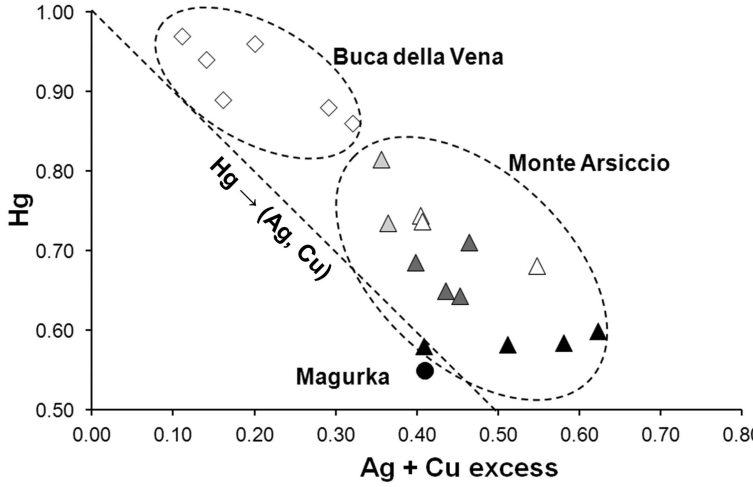

FIG. 4. Hg content (in a.p.f.u.) *vs.* (Ag, Cu) excess in the chemical formulae of rouxelite. Triangles: Monte Arsiccio. Different colours indicate different spot analyses: white = spot analyses A; light grey = spot analyses B; dark grey = spot analyses C; and black = spot analyses D. Rhombs: Buca della Vena mine; circle = Magurka. Tie-line corresponds to Hg = −(Ag,Cu).

TABLE 5. Distribution of (Ag, Cu) and Tl among *Hg* and *Pb* sites, and corrected Pb and Sb contents in the chemical formula of rouxelite.

Sample	Spot	Cu+Ag	Ag,Cu excess	Ag,Cu in Hg	Ag,Cu in Pb	Tl in Pb	Pb corr.	Sb corr.
318	A1	2.40	0.40	0.25	0.15	0.31	22.19	27.81
318	A2	2.55	0.55	0.32	0.23	0.27	22.20	27.80
318	A3	2.41	0.41	0.26	0.14	0.31	22.23	27.77
	Mean A	2.45	0.45	0.28	0.17	0.30	22.21	27.79
318	B1	2.36	0.36	0.18	0.17	0.50	22.25	27.75
318	B2	2.36	0.36	0.26	0.10	0.46	22.18	27.82
	Mean B	2.36	0.36	0.22	0.14	0.48	22.21	27.79
318	C1	2.40	0.40	0.31	0.08	0.83	22.13	27.87
318	C2	2.44	0.44	0.35	0.08	0.87	21.82	28.18
318	C3	2.45	0.45	0.36	0.10	0.91	21.63	28.37
318	C4	2.46	0.46	0.29	0.18	0.71	21.87	28.13
	Mean C	2.44	0.44	0.33	0.11	0.83	21.86	28.14
399	D1	2.51	0.51	0.42	0.09	0.47	21.56	28.44
399	D2	2.58	0.58	0.41	0.17	0.45	21.62	28.38
399	D3	2.62	0.62	0.40	0.22	0.48	22.00	28.00
399	D4	2.41	0.41	0.42	−0.01	0.44	21.62	28.38
	Mean D	2.53	0.53	0.41	0.12	0.46	21.70	28.30
BdV	1	2.29	0.29	0.12	0.17	0.00	23.23	26.77
BdV	2	2.14	0.14	0.06	0.08	0.00	22.98	27.01
BdV	3	2.20	0.20	0.04	0.16	0.00	23.04	26.96
BdV	4	2.32	0.32	0.14	0.18	0.00	23.38	26.62
BdV	5	2.11	0.11	0.03	0.08	0.00	22.98	27.02
BdV	6	2.16	0.16	0.11	0.05	0.00	23.02	26.99
	Mean BdV	2.20	0.20	0.08	0.12	0.00	23.10	26.90
	Magurka	2.41	0.41	0.45	−0.04	0.00	23.17	26.69
	Ideal	2.00	0.00	0.00	0.00	0.00	22.00	28.00

in excess of 1 a.p.f.u. (from 1.07 to 1.18 after subtracting 0.08 Ag in analysis D). This indicates that, while a major amount of the Ag substitutes for Hg (along the tie-line in Fig. 4), a minor amount substitutes for Pb according to the classic heterovalent substitution rule $2Pb^{2+} = Sb^{3+} + Ag^{+}$. Substitution of Hg by Ag (and minor Cu, for analysis C) must be compensated by an equivalent substitution of Pb by Sb, according to the rule $Hg^{2+} + Pb^{2+} = (Ag, Cu)^{+} + Sb^{3+}$. Table 5 indicates the ratios of the (Ag, Cu) excess substituting for Hg and Pb in all rouxelite analyses.

Thallium increases from 0.30 to 0.83 a.p.f.u. and is correlated with Sb, according to Fig. 5*a*. The Sb content is corrected after addition of As and Bi and subtraction of Ag and Cu in excess. The distribution of spot analyses agrees with the tie-line Tl = Sb, starting from an ideal formula of rouxelite. Thallium content is anti-correlated with Pb (Fig. 5*b*), according to the tie-line Tl = −0.5Pb. These two correlations correspond to the incorporation of Tl according to the heterovalent substitution rule $2Pb^{2+} = Sb^{3+} + Tl^{+}$.

Finally, As, not detected in specimens from the type locality and Magurka, substitutes for Sb, ranging between 0.27 and 0.84 a.p.f.u.

The chemical formulae corresponding to the four analyses are:

A: $Cu_{2.00}(Hg_{0.72}Ag_{0.28})_{\Sigma 1.00}Pb_{20.98}(Tl_{0.30}Ag_{0.18})_{\Sigma 0.48}(Sb_{27.87}As_{0.65}Bi_{0.03})_{\Sigma 28.55}S_{65.39}$;

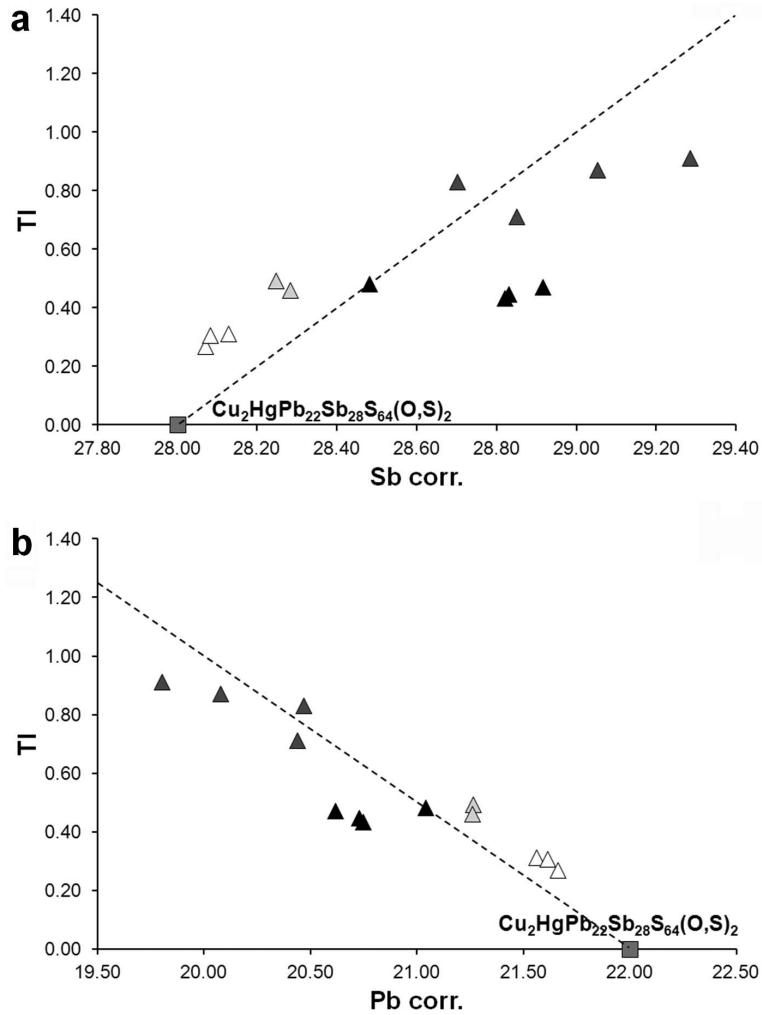

FIG. 5. Tl content (a.p.f.u.) *vs*. Sb content (*a*) and Pb content (*b*) in rouxelite from Monte Arsiccio. In (*a*), Sb corr. = Sb + As + Bi − (Ag, Cu) excess; tie-line corresponds to Tl = Sb, starting from ideal rouxelite, $Cu_2HgPb_{22}Sb_{28}S_{64}(O,S)_2$. In (*b*), Pb corr. = Pb − $(Ag, Cu)_{Hg}$ − $2(Ag, Cu)_{Pb}$; tie-line corresponds to Tl = −0.5Pb, starting from ideal rouxelite. Symbols as in Fig. 4. Square: ideal rouxelite.

B: $Cu_{2.00}(Hg_{0.78}Ag_{0.22})_{\Sigma 1.00}Pb_{20.76}(Tl_{0.48}Ag_{0.14})_{\Sigma 0.62}(Sb_{27.78}As_{0.84})_{\Sigma 28.62}S_{65.43}$;

C: $Cu_{2.00}(Hg_{0.67}Ag_{0.27}Cu_{0.04})_{\Sigma 1.00}Pb_{19.65}(Tl_{0.83}Ag_{0.11})_{\Sigma 0.94}(Sb_{29.13}As_{0.27}Bi_{0.01})_{\Sigma 29.41}S_{65.59}$;

D: $(Cu_{1.92}Ag_{0.08})_{\Sigma 2.00}(Hg_{0.59}Ag_{0.41})_{\Sigma 1.00}Pb_{20.13}(Tl_{0.46}Ag_{0.12})_{\Sigma 0.58}(Sb_{28.60}As_{0.68}Bi_{0.01})_{\Sigma 29.29}S_{66.15}$.

If (Ag, Cu) excess and Tl are subtracted according to the three substitution rules reported above, the corrected values of Pb and Sb (Table 5) are obtained and the four simplified chemical formulae become:

A: $Cu_2HgPb_{22.21}(Sb,As,Bi)_{27.79}S_{65.4}$;
B: $Cu_2HgPb_{22.21}(Sb,As)_{27.79}S_{65.4}$;
C: $Cu_2HgPb_{21.86}(Sb,As,Bi)_{28.14}S_{65.6}$;
D: $Cu_2HgPb_{21.70}(Sb,As,Bi)_{28.30}S_{66.2}$.

In all formulae, the cation ratios fit the ideal formula of rouxelite, $Cu_2HgPb_{22}Sb_{28}S_{64}(O,S)_2$ very well. This ideal formula contains a mixed (O,S) position, but the very low O content

(0.2 wt.% in the type sample) cannot be measured precisely with an electron-microprobe (Orlandi *et al*., 2005). Moreover, the uncertainty on the S ratio in the four structural formulae do not allow the O ratio by difference on the basis of 66 anions (the S ratio overpasses this value in analysis D) to be obtained.

Rouxelite from Buca della Vena shows a small Cu excess, with respect to the studied specimens, which substitutes for Hg and also Pb (Fig. 4), whereas Hg is replaced by Ag at Magurka (~33 at.%, together with ~8 at.% Cu) and Monte Arsiccio (up to 40 at.% in analysis D). This large substitution by Ag confirms the explanation proposed by Orlandi *et al*. (2005) for the incorporation of Ag in rouxelite from Magurka. In fact, as noted by these authors, the bonding environment of the *Hg* site in rouxelite is the same as observed for Ag in neyite, $Ag_2Cu_6Pb_{25}Bi_{26}S_{68}$ (Makovicky *et al*., 2001).

The presence of Tl (up to 1.81 wt.% in the C3 spot analysis, corresponding to 0.91 a.p.f.u.) is the most specific feature of rouxelite from Monte Arsiccio, agreeing with the Tl-rich nature of the Monte Arsiccio mineral assemblage. Indeed, rouxelite is associated with Tl-bearing varieties of robinsonite and chovanite (under study). Thallium is probably concentrated at the Pb positions having the highest coordination number (C.N. = 8) due to the large size of the Tl^+ cation in the crystal structure of rouxelite. Unfortunately, owing to the low diffraction quality of the crystals available, it was not possible to establish whether Tl is distributed among several Pb positions, or if it occupies a specific site.

There is no correlation between Tl and Ag substituting for Pb in rouxelite from Monte Arsiccio according to Table 5, thus indicating that Tl and Ag are probably incorporated into distinct *Pb* sites. Finally, the presence of As in the rouxelite studied agrees with the presence of As minerals in the Monte Arsiccio mineral assemblage (arsenopyrite, realgar, complex Hg-Tl-As phases).

Curiously, unlike rouxelite from Monte Arsiccio, the Pb/Sb corrected ratios of rouxelite from Buca della Vena and Magurka (Table 5) fit the 23/27 ratio very well but not the ideal 22/28 ratio. Such a discrepancy is difficult to explain, according to the accuracy of microprobe analysis. A comparative crystal-structure study would be necessary to solve this question.

Copper-mercury and silver-mercury substitutions in natural sulfides and sulfosalts

As described in the previous paragraph, in rouxelite, Hg^{2+} can be replaced by Ag^+ (specimens from Magurka and Monte Arsiccio) and Cu^+ (type specimen from Buca della Vena). These substitutions take place at the *Hg* site, consequently giving a mixed (Hg,Ag) or (Hg,Cu) occupancy. These kinds of occupancy have been observed in a few other natural sulfosalts, the crystal chemistry of which is discussed here.

Chen and Szymański (1981, 1982) observed a mixed (Hg,Cu,Zn) tetrahedral site in the crystal structure of galkhaite and reported a +2 valence state for Cu. Such a valence attribution is questionable. Indeed, if the full occupancy of the trigonal pyramidal *As* site is assumed, as suggested by the crystal structure study (Chen and Szymański, 1981), the ideal chemical formula of galkhaite may be written as $(Hg,Cu)_6(Cs,Tl)As_4S_{12}$. If one assumes a formal valence of +2 for Hg and Cu, +1 for Cs and Tl and +3 for As, there is an excess of positive charges. Examination of the chemical analyses reported by Chen and Szymański (1981, 1982) for galkhaite from the Getchell mine, Nevada, USA and Khaydarkan, Kyrgyzstan, points to an average composition of the tetrahedral site $[(Hg,Zn)^{2+}_{4.9(1)}(Cu,Ag)^{+}_{0.9(1)}]_{\Sigma=5.8(2)}$. In galkhaite from the Getchell mine, the sum (Cs + Tl) is 0.88(3) a.p.f.u., whereas in the specimens from Khaydarkan the sum of (Cs + Tl) is significantly smaller, i.e. 0.50(1) a.p.f.u. Chen and Szymański (1982) hypothesized the occurrence of Rb^+ in galkhaite from this latter occurrence, but they did not detect this alkaline metal. These data agree with new electron-microprobe analyses performed by Pekov and Bryzgalov (2006) on specimens from different occurrences; only one sample from the Kara-Archa area, Khaidarkan, Kyrgyzstan, showed a total (Cs + Tl) = 0.50 a.p.f.u., whereas all the other samples analysed gave totals ranging from 0.84 to 0.99 a.p.f.u. If a full occupancy of the (Cs,Tl)-centred site is assumed, a valence state could be hypothesized of +1 for Cu and the substitution of Hg^{2+} by Cu^+ would be a case of valency-imposed double-site occupancy (Hatert and Burke, 2008), related to the introduction of a monovalent large cation in the structure, i.e. Cs^+, Tl^+. If so, the correct crystal-chemical formula of galkhaite should be written as $(Hg_{5+x}Cu_{1-x})(Cs,Tl)_{1-x}As_4S_{12}$. Consequently,

further chemical studies on galkhaite from Khaydarkan are mandatory in order to solve the chemical uncertainties related to the deficit of large monovalent cations. Moreover, the possible substitution of these cations by K^+ or $(NH_4)^+$ ions, as observed in ambrinoite (Biagioni *et al*., 2011), should be kept in mind.

If the heterovalent substitution $Hg^{2+} \leftrightarrow Cu^+$ takes place, an excess or a deficit of charges is produced and consequently another substitution must occur. In aktashite, Biagioni *et al*. (2013*a*) proposed a cross-substitution between the two tetrahedral sites *Hg* and *Cu*2, with Hg^{2+} partially replaced mainly by Cu^+ at the *Hg* site and Cu^+ being replaced mainly by Hg^{2+} at the *Cu*2 site. Moreover, the $Hg^{2+} \rightarrow Cu^+$ substitution has been observed in the linearly coordinated *Hg* site of fettelite by Bindi *et al*. (2012); in order to maintain the electrostatic balance, another substitution must occur, with Ag^+ substituted by a divalent cation (e.g. Zn^{2+}).

Among sulfosalts, mixed (Hg,Ag) sites have also been observed in arsiccioite (Biagioni *et al*., 2014), ideally $^{M1}Hg^{M2}(Hg_{0.5}Ag_{0.5})_2TlAs_2S_6$ in addition to rouxelite. The substitution of Hg^{2+} by Ag^+ at the *M*2 site is coupled with the replacement of an equal amount of $(Cu,Ag)^+$ by Hg^{2+} at the *M*1 site. A mixed (Hg,Ag) site was reported by Mumme and Nickel (1987) for the sulfide mineral perroudite, $Hg_{4.6}Ag_{4.4}S_{4.6}(Cl_{2.0}Br_{0.8}I_{1.6})$. In this case, the site occupancy of the mixed (Hg,Ag) site is controlled by the heterovalent substitution $Hg^{2+} + S^{2-} = Ag^+ + (Cl,Br,I)^-$.

Conclusion

Rouxelite from Monte Arsiccio represents the third occurrence of this complex Pb-Sb sulfosalt. It shows a more complex crystal chemistry, compared to the neighbouring occurrence of Buca della Vena, reflecting the complexity of the ore geochemistry at Monte Arsiccio. In particular, rouxelite from this locality constitutes a new example of a Tl-bearing sulfosalt. Some crystal-chemical characteristics of rouxelite remain to be refined by new crystal-structure studies, like the effective Pb/Sb ideal atomic ratio (23/27 or 22/28?), or the localization of Tl among Pb positions.

Acknowledgements

Electron-microprobe analyses were performed with the help of J. Langlade (CNRS ingeneer, 'Microsonde Ouest' laboratory, IFREMER, Plouzané, France). Comments by Luca Bindi, Andrea Dini and Stephan Graeser helped to improve the paper.

References

Biagioni, C., Bonaccorsi, E., Pasero, M., Moëlo, Y., Ciriotti, M.E., Bersani, D., Callegari, A.M. and Boiocchi, M. (2011) Ambrinoite, $(K,NH_4)_2(As,Sb)_8S_{13}\cdot H_2O$, a new mineral from the Upper Susa Valley, Piedmont, Italy: The first natural (K,NH_4)-hydrated sulfosalt. *American Mineralogist*, **96**, 878–887.

Biagioni, C., Bonaccorsi, E., Moëlo, Y. and Orlandi, P. (2013*a*) Mercury-arsenic sulfosalts from the Apuan Alps (Tuscany, Italy). III. Aktashite, $Cu_6Hg_3As_4S_{12}$, and laffittite, $AgHgAsS_3$, from the Monte Arsiccio mine: occurrence and crystal structure. *Periodico di Mineralogia*, **83**, 1–18.

Biagioni, C., D'Orazio, M., Vezzoni, S., Dini, A. and Orlandi, P. (2013*b*) Mobilization of Tl-Hg-As-Sb-(Ag,Cu)-Pb sulfosalt melts during low-grade metamorphism in the Alpi Apuane (Tuscany, Italy). *Geology*, **41**, 747–751.

Biagioni, C., Moëlo, Y., Orlandi, P., Stanley, C.J. and Evain, M. (2013*c*) Meerschautite, IMA 2013-061. CNMNC Newsletter No. 17, October 2013, page 3004; *Mineralogical Magazine*, **77**, 2997–3005.

Biagioni, C., Orlandi, P. and Moëlo, Y. (2013*d*) Carducciite, IMA 2013-006. CNMNC Newsletter No. 16, August 2013, page 2702; *Mineralogical Magazine*, **77**, 2695–2709.

Biagioni, C., Bonaccorsi, E., Moëlo, Y., Orlandi, P., Bindi, L., D'Orazio, M. and Vezzoni, S. (2014) Mercury-arsenic sulfosalts from the Apuan Alps (Tuscany, Italy). II. Arsiccioite, $AgHg_2TlAs_2S_6$, a new mineral from the Monte Arsiccio mine: occurrence, crystal structure and crystal chemistry of the routhierite isotypic series. *Mineralogical Magazine*, **78**, 101–117.

Bindi, L., Downs, R.T., Spry, P.G., Pinch, W.W. and Menchetti, S. (2012) A chemical and structural re-examination of fettelite samples from the type locality, Odenwald, southwest Germany. *Mineralogical Magazine*, **76**, 551–566.

Chen, T.T. and Szymański, J.T. (1981) The structure and chemistry of galkhaite, a mercury sulfosalt containing Cs and Tl. *The Canadian Mineralogist*, **19**, 571–581.

Chen, T.T. and Szymański, J.T. (1982) A comparison of galkhaite from Nevada and from the type locality, Khaydarkan, Kirgizia, U.S.S.R.. *The Canadian Mineralogist*, **20**, 575–577.

Costagliola, P., Benvenuti, M., Tanelli, G., Cortecci, G. and Lattanzi, P. (1990) The barite-pyrite-iron oxides

deposit of Monte Arsiccio (Apuane Alps). Geological setting, mineralogy, fluid inclusions, stable isotopes and genesis. *Bollettino della Società Geologica Italiana*, **109**, 267–277.

Hatert, F. and Burke, E.A.J. (2008) The IMA-CNMNC dominant-constituent rule revisited and extended. *The Canadian Mineralogist*, **46**, 717–728.

Laugier, J. and Bochu, B. (1999) *CELREF: Cell parameters refinement program from powder diffraction diagram*. Laboratoire des Matériaux et du Génie Physique, Ecole Nationale Supérieure de Physique de Grenoble (INPG), Grenoble, France.

Makovicky, E., Balić-Žunić, T. and Topa, D. (2001) The crystal structure of neyite, $Ag_2Cu_6Pb_{25}Bi_{26}S_{68}$. *The Canadian Mineralogist*, **39**, 1365–1376.

Moëlo, Y., Makovicky, E., Mozgova, N.N., Jambor, J.L., Cook, N., Pring., A., Paar, W.H., Nickel, E.H., Graeser, S., Karup-Møller, S., Balić-Žunić, T., Mumme, W.G., Vurro, F., Topa, D., Bindi, L., Bente, K. and Shimizu, M. (2008) Sulfosalt systematics: a review. Report of the sulfosalt subcommittee of the IMA Commission on Ore Mineralogy. *European Journal of Mineralogy*, **20**, 7–46.

Moëlo, Y., Orlandi, P., Guillot-Deudon, C., Biagioni, C., Paar, W. and Evain, M. (2011) Lead-antimony sulfosalts from Tuscany (Italy). XI. The new mineral species parasterryite, $Ag_4Pb_{20}(Sb_{14.5}As_{9.5})_{\Sigma 24}S_{58}$, and associated sterryite, $Cu(Ag,Cu)_3Pb_{19}(Sb,As)_{\Sigma 22}(As–As)S_{56}$, from the Pollone mine, Tuscany, Italy. *The Canadian Mineralogist*, **49**, 623–638.

Mumme, W.G. and Nickel, E.H. (1987) Crystal structure and crystal chemistry of perroudite: A mineral from Coppin Pool, Western Australia. *American Mineralogist*, **72**, 1257–1262.

Orlandi, P., Moëlo, Y., Meerschaut, A. and Palvadeau, P. (1999) Lead-antimony sulfosalts from Tuscany (Italy). I. Scainiite, $Pb_{14}Sb_{30}S_{54}O_5$, the first Pb-Sb oxy-sulfosalt, from Buca della Vena mine. *European Journal of Mineralogy*, **11**, 949–954.

Orlandi, P., Moëlo, Y., Meerschaut, A., Palvadeau, P. and Léone, P. (2005) Lead-antimony sulfosalts from Tuscany (Italy). VIII. Rouxelite, $Cu_2HgPb_{22}Sb_{28}S_{64}(O,S)_2$, a new sulfosalt from Buca della Vena mine, Apuan Alps: definition and crystal structure. *The Canadian Mineralogist*, **43**, 919–933.

Orlandi, P., Biagioni, C., Bonaccorsi, E., Moëlo, Y. and Paar, W. (2012) Lead-antimony sulfosalts from Tuscany (Italy). XII. Boscardinite, $TlPb_4(Sb_7As_2)_{\Sigma 9}S_{18}$, a new mineral species from the Monte Arsiccio mine: occurrence and crystal structure. *The Canadian Mineralogist*, **50**, 235–251.

Orlandi, P., Biagioni, C., Moëlo, Y., Bonaccorsi, E. and Paar, W. (2013) Lead-antimony sulfosalts from Tuscany (Italy). XIII. Protochabournéite, $\sim Tl_2Pb(Sb_{9-8}As_{1-2})_{\Sigma 10}S_{17}$, from the Monte Arsiccio mine: occurrence, crystal structure and relationship with chabournéite. *The Canadian Mineralogist*, **51**, 475–494.

Pandeli, E., Bagnoli, P. and Negri, M. (2004) The Fornovolasco schists of the Apuan Alps (Northern Tuscany, Italy): a new hypothesis for their stratigraphic setting. *Bollettino della Società Geologica Italiana*, **123**, 53–66.

Pekov, I.V. and Bryzgalov, I.A. (2006) New data on galkhaite. *New Data on Minerals*, **41**, 26–32.

Topa, D., Sejkora, J., Makovicky, E., Pršek, J., Ozdín, D., Putz, H., Dittrich, H. and Karup-Møller, S. (2012) Chovanite, $Pb_{15-2x}Sb_{14+2x}S_{36}O_x$ (x~0.2), a new sulphosalt species from the Low Tatra Mountains, Western Carpathians, Slovakia. *European Journal of Mineralogy*, **24**, 727–740.